Theor Chem Acc (2001) 105:477–480
DOI 10.1007/s002140000238

Theoretical
Chemistry Accounts

Letter

Transition state for intramolecular C–H bond cleavage in $[(L\text{Cu})_2(\mu\text{-O})_2]^{2+}$ (L = 1,4,7-tribenzyl-1,4,7-triazacyclononane)

Christopher J. Cramer, Youngshang Pak[1]

Department of Chemistry and Supercomputer Institute, University of Minnesota, 207 Pleasant St. SE, Minneapolis, MN 55455–0431, USA
e-mail: cramer@chem.umn.edu

Received: 10 October 2000 / Accepted: 3 November 2000 / Published online: 3 April 2001

Abstract. Hybrid quantum mechanical/molecular mechanical electronic structure calculations reveal the transition state for C–H bond cleavage in $[(L\text{Cu})_2(\mu\text{-O})_2]^{2+}$ (L = 1,4,7-tribenzyl-1,4,7-triazacyclononane) to be consistent with a hydrogen-atom-transfer mechanism from carbon to oxygen. At the MPW1K/double-zeta effective core potential(+)|univeral force field level, 0 K activation enthalpies for the parent, *p*-CF3, and *p*-OH substituted benzyl systems are predicted to be 8.8, 9.5, and 7.8 kcal/mol. Using a one-dimensional Eckart potential to estimate quantum effects on the reaction coordinate, reaction in the unsubstituted system is predicted to proceed with a primary kinetic isotope effect of 22 at 233 K. Structural parameters associated with the hydrogen-atom transfer are consistent with the Hammond postulate.

Key words: Binuclear copper – Oxygen activation – Tunneling – C–H activation – Hydrogen-atom transfer

Copper complexes that activate molecular oxygen have attracted substantial recent attention both because of their presence in certain metalloenzymes and because of their potential utility for aliphatic C–H bond activation [1–3]. The oxidizing power of two particular coordination geometries for oxygen has been established, namely for the isomeric μ-η^2:η^2-peroxo- and bis(μ-oxo)dicopper motifs. Halfen et al. [4] have demonstrated that under certain conditions these two coordination geometries can be in rapid equilibrium, with the equilibrium constant being quite sensitive to the nature of the other ligands coordinating copper. The existence of this equilibrium raises a fundamental mechanistic question: Which isomeric form is responsible for hydrocarbon C–H bond activation, for example, the aromatic hydroxylation performed by tyrosinase [1, 5, 6]? Studies of synthetic μ-η^2:η^2-peroxo complexes indicate that this form is capable of hydroxylating a suitably disposed arene [7], but the predominant reaction pathway for bis(μ-oxo) systems (with a few exceptions [5, 8]) is intramolecular hydroxylation at the C–H bond of supporting ligand substituents; this ultimately yields *N*-dealkylated product(s) in most cases (Fig. 1) [9, 10]. This reaction is of great interest in its own right since it is relevant to a wide range of hydrocarbon oxidations carried out by metalloproteins and synthetic reagents [11–13], and it therefore warrants detailed mechanistic analysis. In experimental studies [9, 14, 15] very large primary kinetic isotope effects (KIEs) have been observed in *N*-dealkylation reactions of bis-μ-oxo complexes, leading to postulates of a rate-determining step with substantial heavy-atom–hydrogen bond-order changes. These and other data have been cited to support a hydrogen-atom transfer path, but other possibilities merit consideration, including hydride transfer, coupled or decoupled proton transfer/electron transfer, and direct oxygen-atom insertion into the C–H bond.[1]

To offer more insight into the structure of the transition state (TS) associated with the rate-determining step, we have carried out large-scale electronic-structure calculations on the system of Mahapatra et al. [9] (Scheme 1). Employing the integrated molecular orbital molecular mechanics (IMOMM) formalism of Maseras and Morokuma [17], we treat the five "spectator" benzyl groups at the MM level using the universal force field (UFF) [18]. All remaining atoms are treated with unrestricted density functional theory using the MPW1K functional [19] and a double-zeta (DZ) effective-core-

---

Present address[1]:
Department of Chemistry, Pusan National University,
College of Natural Sciences, Kumjeong-ku,
Pusan 609-735, Korea

[1] We note that the intramolecular nature of the C–H bond activation studied here is distinct from the intermolecular activation present in, say, tyrosinase. For computational studies on tyrosinase itself and smaller models see Ref. [16].

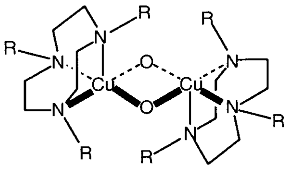

1, **a:** R = PhCH$_2$
b: R = p-CF$_3$PhCH$_2$
c: R = p-HOPhCH$_2$

Scheme 1

potential (ECP) basis set [20, 21] with diffuse functions added to the O and C atoms involved in the hydrogen-atom transfer. We denote this level of theory as MPW1K/DZ-ECP(+)|UFF. The MPW1K functional [19] is a modification of the MPW1PW91 functional [22] where the percentage of Hartree–Fock exchange has been optimized for accuracy in reproducing the energetics of well characterized hydrogen-atom transfer reactions.

We have identified fully optimized reactant (R), intermediate product (P), and TS structures for a reaction coordinate of **1a** corresponding to hydrogen transfer from C to O (Fig. 2). All species are singlets. The nature

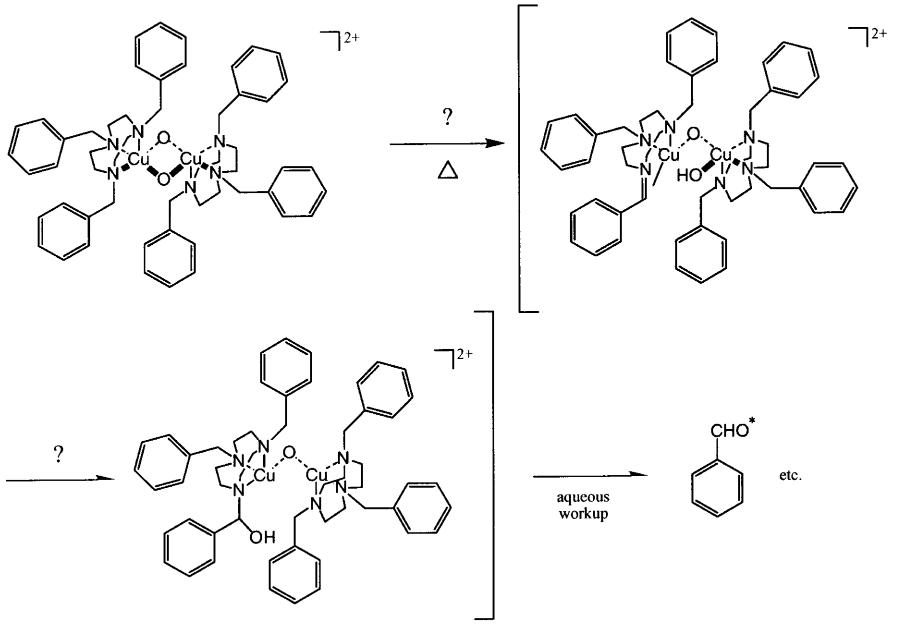

Fig. 1. Oxidative dealkylation pathway for $[(L\mathrm{Cu})_2(\mu\text{-O})_2]^{2+}$ (L = 1,4,7-tribenzyl-1,4,7-triazacyclononane) with hypothetical reactive intermediates in brackets. Labeling studies have confirmed the intramolecular nature of the ultimate oxygen-atom transfer

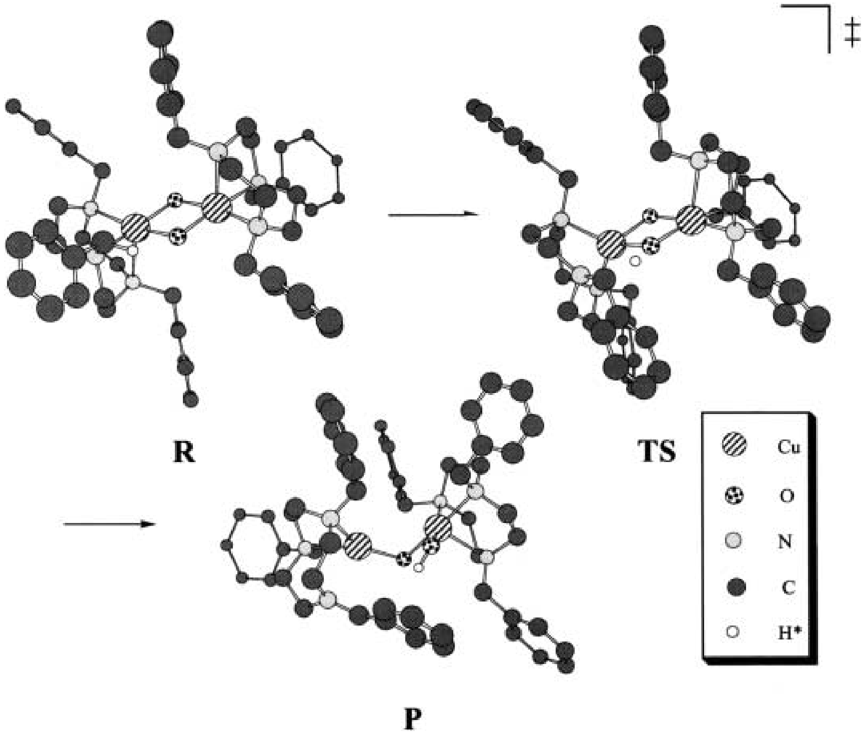

Fig. 2. Ball-and-stick structures for reactant (R), transition state (TS), and intermediate product (P) of **1a** computed at the MPW1K/double-zeta (DZ)–effective-core-potential (ECP)(+)|universal force field (UFF) level. All hydrogen atoms other than the one in flight (H*) have been deleted for clarity

of each stationary point has been confirmed by analytic frequency calculations, which have also been used for thermochemical calculations. The degree of hydrogen transfer is quite advanced in the TS structure, with the breaking C–H bond at 1.310 Å and the forming O–H bond at 1.217 Å (Table 1). The predicted 0 K enthalpy of activation is 8.8 kcal/mol. This is somewhat below the experimentally determined activation enthalpy of 13.0 ± 0.5 kcal/mol for the perchlorate salt in CH_2Cl_2. The difference is attributable in part to practical limitations restricting to double-zeta the size of the employed basis set; counterion and solvation effects may certainly also contribute to the difference. The reaction exothermicity is predicted to be 22.6 kcal/mol.

Mahapatra et al. [9] have also provided experimental data for *para*-substituted analogs of **1a**. Our computations on **1b** and **1c** indicate the activation enthalpies for hydrogen transfer in these systems to be increased and decreased relative to **1a** by 0.7 and 1.0 kcal/mol, respectively. Experimentally, these values are 0.3 and 0.4, respectively for the *p*-CF3 and *p*-OCH_3 substituted systems. As expected, the agreement between theory and experiment is better for such relative comparisons than for the absolute barrier. The somewhat larger sensitivity to substitution exhibited by the calculations probably reflects a modest leveling effect in solution compared to the gas phase.

Table 1. Transition state properties of **1a**, **b**, and **c** at the MPW1K/double-zeta–effective-core-potential(+)|univeral force field level

Property	1a	1b	1c
*r*Cu–Cu, Å	2.943	2.947	2.944
*r*O–O, Å	2.257	2.253	2.251
*r*C–H*, Å	1.310	1.325	1.298
*r*O–H*, Å	1.217	1.203	1.233
∠C–H*–O, degree	142.4	142.2	142.4
$\Delta H_0^{\ddagger}$, kcal/mol	8.8	9.5	7.8

To provide additional validation of the relevance of the computed TS structure, we computed the primary KIE associated with the reaction coordinate for **1a**. Quantum effects on the reaction coordinate were estimated by fitting the zero-point-including potential energy and imaginary frequency (H: 1109*i*; D: 874*i*) to a one-dimensional Eckart potential [23] and solving the relevant Schrödinger equation [24]. The predicted KIE at 233 K is 22, while the experimental [9] value for the perchlorate salt in solution is 40 ± 4 (using the experimental activation enthalpy instead of the theoretical one has little effect on the computed KIE). The factor of 2 difference between theory and experiment is consistent with the error expected from considering only one-dimensional tunneling, although condensed-phase effects may also play a role. We note that the classical KIE is predicted to be only 8.3.

Given these agreements between theory and experiment for absolute and relative energetics, and for barrier shape (as judged by the tunneling and KIE calculations), we consider the predicted TS structure to be the relevant one for the experimentally observed oxidative dealkylations. Geometrical analysis (Table 1, Fig. 3) indicates the TS to be well described as a bis-*μ*-oxo species (typical bis-*μ*-oxo Cu–Cu and O–O bond lengths are 2.8 and 2.3 Å, respectively [14, 25, 26]), i.e., there is no significant peroxo character (typical peroxo Cu–Cu and O–O bond lengths are 3.6 and 1.4 Å, respectively [27]). Moreover, there is no oxygen-atom insertion character. Indeed, attempts to force oxygen-insertion by driving the C–O bond distance inevitably led either to hydrogen transfer or to unreasonably high-energy species. These calculations do not, of course, rule out the possibility that there is also a peroxo-like TS with a similar barrier height and shape, in which case if conversion between bis-*μ*-oxo and peroxo motifs proceeds with a lower

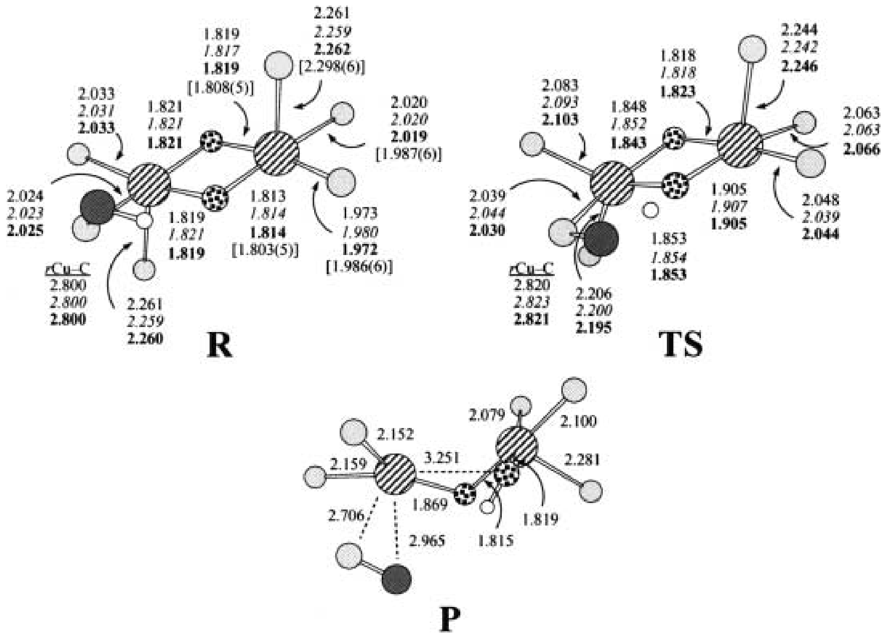

Fig. 3. Ball-and-stick structures at the MPW1K/DZ–ECP(+)|UFF level for the cores of R, TS, and P with the same orientation as in Fig. 2. Key heavy atom distances are labeled for computed **1a** (roman), **1b** (italic), **1c** (boldface), and experimental **1a** (in brackets, from X-ray crystallography, Ref. [24])

barrier than hydrogen-atom abstraction, the reaction could proceed via both pathways. Occam's razor suggests, however, that this is unlikely.

We note that the hydrogen transfer takes place from an equatorial benzyl group (Figs. 1, 2). The C–H and O–H distances in **1a**, **b**, and **c** vary in a manner consistent with the Hammond postulate [28]; the TS structure is most reactant-like in **1c**, which has the lowest barrier, and most product like in **1b**, which has the highest barrier. Interestingly, when we attempted to induce oxidation of an axially located benzyl group by enforcing reduced O–H distances, the entire triazacyclononane ligand rotated to move the benzyl group to an equatorial position prior to hydrogen transfer. Low barriers to ligand rearrangement in analogous bis-μ-oxo complexes have been previously computed and are consistent with experimental spectroscopic data [25]. Even in the equatorial position, the hydrogen transfer involves a large deviation of the three relevant atoms from collinearity, suggesting that barriers for analogous intermolecular oxidations by bis-μ-oxo complexes, where collinear arrangements would be expected to be more accessible, may be substantially lower than is the case for intramolecular cases [15].

Theory also permits an analysis of the polarity of the hydrogen transfer. A simple Mulliken population analysis indicates the hydrogen atom in flight to be more negatively charged in the TS structure than in the reactant, but by only 0.003, 0.004, and 0.007 charge units in **1a**, **b**, and **c**, respectively. This negligible change in hydrogen charge suggests that this TS is well described as a hydrogen-atom transfer. The product structure suggests, however, that later along the reaction coordinate there is rehybridization of the *N*-benzyl radical fragment to an iminium ligand which weakly π coordinates to a (reduced) copper(II) atom. Internal hydroxyl delivery back to the oxidized carbon would then amount to an intramolecular nucleophilic addition rather than radical–radical recombination. Theoretical characterization of this subsequent step is ongoing.

Acknowledgements. We thank the Army Research Office and the National Science Foundation for financial support, the Minnesota Supercomputer Institute for HPC resources and Bill Tolman for penetrating insights.

References

1. Solomon EI, Sundaram UM, Machonkin TE (1996) Chem Rev 96: 2563
2. Kopf M-A, Karlin KD (2000) In: Meunier B (ed) Biomimetic oxidations catalyzed by transition metal complexes. Imperial College Press, London, p 309
3. Blackman AG, Tolman WB (2000) In: Meunier B (ed) Metal–oxo and metal–peroxo species in catalytic oxidations. Springer, Berlin Heidelberg New York, p 179
4. Halfen JA, Mahapatra S, Wilkinson EC, Kaderli S, Young VG, Que L, Zuberbühler AD, Tolman WB (1996) Science 271: 1397
5. Holland PL, Rodgers KR, Tolman WB (1999) Angew Chem Int Ed Engl 38: 1139
6. (a) Monzani E, Quinti L, Perotti A, Casella L, Gullotti M, Randaccio L, Geremia S, Nardin G, Faleschini P, Tabbì G (1998) Inorg Chem 37: 553; (b) Monzani E, Battaini G, Perotti A, Casella L, Gullotti M, Santagostini L, Nardin G, Randaccio L, Geremia S, Zanello P, Opromolla G (1999) Inorg Chem 38: 5359; (c) Decker H, Dillinger R, Tuczek F (2000) Angew Chem Int Ed Engl 39: 1591
7. Pidcock E, Obias HV, Zhang CX, Karlin KD, Solomon EI (1998) J Am Chem Soc 120: 7841, and references therein
8. Mahadevan V, DuBois JL, Hedman B, Hodgson KO, Stack TDP (1999) J Am Chem Soc 121: 5583
9. Mahapatra S, Halfen JA, Tolman WB (1996) J Am Chem Soc 118: 11575
10. Tolman WB (1997) Acc Chem Res 30: 227
11. Groves JT, Han Y-Z (1995) In: de Montellano PRO (ed) Cytochrome P450: stucture, mechanism, and biochemistry, 2nd edn. Plenum, New York, p 3
12. Mayer JM (1998) Acc Chem Res 31: 441
13. Meunier B (ed) (2000) Biomimetic oxidations catalyzed by transition metal complexes. Imperial College Press, London
14. Mahadevan V, Hou Z, Cole AP, Root DE, Lal TK, Solomon EI, Stack TDP (1997) J Am Chem Soc 119: 11996
15. Itoh S, Taki M, Nakao H, Holland PL, Tolman WB, Que L, Fukuzumi S (2000) Angew Chem Int Ed Engl 39: 3398
16. (a) Eisenstein O, Getlicherman H, Giessner-Prettre C, Maddaluno J (1997) Inorg Chem 36: 3455; (b) Lind T, Siegbahn PEM, Crabtree RH (1999) J Phys Chem B 103: 1193
17. Maseras F, Morokuma K (1995) J Comput Chem 16: 1170
18. (a) Rappé AK, Casewit CJ, Colwell KS, Goddard WA III, Skiff WM (1992) J Am Chem Soc 114: 10024; (b) Rappé AK, Casewit CJ, Colwell KS, Goddard WA III, Skiff WM (1992) J Am Chem Soc 114: 10035; (c) Rappé AK, Casewit CJ, Colwell KS, Goddard WA III, Skiff WM (1992) J Am Chem Soc 114: 10046
19. Lynch BJ, Fast PL, Harris M, Truhlar DG (2000) J Phys Chem A 104: 4811
20. Dunning TH, Hay PJ (1977) In: Schaefer HF III (ed) Methods of electron structure theory. Plenum, New York, p 1
21. Hay PJ, Wadt WR (1985) J Chem Phys 82: 270
22. Adamo C, Barone V (1998) J Chem Phys 108: 664
23. Eckart C (1930) Phys Rev 34: 1303
24. Steinfeld JI, Francisco JS, Hase WL (1999) Chemical kinetics and dynamics, 2nd edn. Prentice-Hall, New York
25. Mahapatra S, Halfen JA, Wilkinson EC, Pan G, Wang X, Young VG, Cramer CJ, Que L, Tolman WB (1996) J Am Chem Soc 118: 11555
26. Mahapatra S, Young VG, Kaderli S, Zuberbühler AD, Tolman WB (1997) Angew Chem Int Ed Engl 36: 1301
27. Kitajima N, Fujisawa K, Fujimoto C, Moro-oka Y, Hashimoto S, Kitagawa T, Toriumi K, Tatsumi K, Nakamura A (1992) J Am Chem Soc 114: 1277
28. Hammond GS (1955) J Am Chem Soc 77: 334